# Magnetic ordering in nanocrystalline gadolinium: A neutron diffraction study

D. H. Ryan
*Physics Department and Centre for the Physics of Materials, McGill University, 3600 University Street, Montreal, Quebec, Canada H3A 2T8*

A. Michels and F. Döbrich
*Laboratory for the Physics of Advanced Materials, University of Luxembourg, 162A Avenue de la Faïencerie, L-1511 Luxembourg, Luxembourg*

R. Birringer
*Experimentalphysik, Universität des Saarlandes, Postfach 151150, D-66041 Saarbrücken, Germany*

Z. Yamani
*National Research Council Canadian Neutron Beam Centre, Chalk River, Ontario, Canada K0J 1J0*

J. M. Cadogan
*School of Physical, Environmental and Mathematical Sciences, University of New South Wales Canberra at the Australian Defence Force Academy, P.O. Box 7916, Canberra, Australian Capital Territory, BC 2610, Australia*
(Received 12 December 2012; published 8 February 2013)

The magnetic ordering of nanocrystalline gadolinium (crystallite sizes of 21 nm and 38 nm) has been studied using neutron diffraction and compared with that of a reference ($\sim$1 $\mu$m) sample. In contrast with bulk gadolinium in which the moments order initially parallel to the $c$-axis and then cant by as much as 60° away from the $c$-axis below 250 K, before rotating back towards the $c$-axis on further cooling, both nanocrystalline samples order with their moments canted by about 50° from the $c$-axis, and this canting angle is largely temperature independent.

DOI: 10.1103/PhysRevB.87.064408 PACS number(s): 75.50.Tt, 61.05.fm, 75.25.−j

## I. INTRODUCTION

While the half-filled $4f$ shell ($L = 0$; $J = S = \frac{7}{2}$) should make gadolinium metal one of the simplest of the magnetic rare-earth systems, it still continues to attract interest. The saturation moment ($T = 0$) of 7.63 $\mu_B$ reflects a significant (0.63 $\mu_B$) contribution from conduction band polarization (in addition to the 7 $\mu_B$ local moment from the Gd $4f$ shell), and spin-orbit coupling between the local $4f$ Gd moments and the polarized conduction electrons leads to the majority of the observed magnetic anisotropy energy in gadolinium metal.[1] This anisotropy is the most likely source of the surprisingly complex magnetic ordering behavior of this "simple" system. Neutron diffraction[2] and magnetization measurements[3] showed that gadolinium does not adopt a helimagnetic structure (common in many of the heavy rare earths) at any temperature, however, the $c$-axis ferromagnetic order that appears at $T_c \sim 293$ K is followed by a reorientation that starts at $T_{sr} \sim 232$ K as the moments cant away from the $c$ axis by more than 60° at 180 K before returning to about 30° off the $c$ axis as $T \to 0$ (Ref. 4). This sequence of ordering and spin rotation has been confirmed in complete detail by torque magnetometry,[5] and is also seen by muon spin relaxation ($\mu SR$) (Ref. 6).

$T_{sr}$ decreases more rapidly in response to hydrostatic pressure than $T_c$, with $dT_{sr}/dP = -42(3)$ K/GPa (Ref. 7) compared with $dT_c/dP = -14.5(7)$ K/GPa (Refs. 8,9). This suggests that the anisotropy energy is more strongly affected by pressure than the overall exchange energy, a view that was confirmed by torque measurements.[10] With $L = 0$, the closed-shell gadolinium ion has no spin-orbit coupling for the $4f$ electrons (to first order), and as noted above, the bulk of the anisotropy energy therefore derives from the polarized conduction electrons. The large $dT_{sr}/dP$ and rapid drop in anisotropy suggests that the anisotropy is associated with one or more sharp features in the density of states, and recent first-principles calculations support this conclusion.[1]

The current interest in nanocrystalline materials and application of the inert-gas condensation technique[11] to rare earths such as terbium[12] and gadolinium[13] has opened up the influence of a new parameter—grain size—and its impacts on the ordering and anisotropy of gadolinium. The simplest impact of reducing the grain size is to place the interior of the grain under pressure. Where this has been studied in nanocrystalline Pd, for interface stresses of 1–10 N/m and a grain size of 20 nm, the internal pressure (relative to hydrostatic pressure outside) is of the order of a few GPa (Ref. 14). Changes in both $T_c$ (Ref. 15) and anisotropy[16] have been attributed to the effects of interface stresses from grain boundaries. As the grains become smaller, a larger fraction of the atoms are located at the surfaces, in grain boundary regions, and by 10 nm, $\sim$30% of the atoms lie on the boundaries, in regions where disorder dominates. The grain-boundary component can be seen by $^{155}$Gd Mössbauer spectroscopy[16] where it appears as a distinct, low-field contribution in the spectra. Grain-boundary-induced spin disorder also shows up in small-angle neutron scattering (SANS) measurements[17–19] where significant spin-misalignment scattering is observed, even in fields of several tesla, with the long-range disorder being more easily suppressed than the nanoscale disorder. It is clear that the disorder in the grain boundaries leads to significant local anisotropy effects, even in gadolinium.

We extend the SANS investigation of nanocrystalline gadolinium (nc-Gd) by looking at one of the simplest local

 

magnetic parameters: the easy axis. Working with two $^{160}$Gd samples from a previous study [a coarse-grained "bulk" reference sample and one with a grain size of 21 nm (Ref. 19)] and a newly prepared 38-nm sample, we have used neutron diffraction to determine the temperature dependence of the magnetic ordering direction. The reference sample closely follows the reorientation behavior described by Cable and Wollan,[4] however, the ordering direction in both nc-Gd samples is largely independent of temperature, with the moments canted by 40°–50° from the $c$ axis from $T_c$ down to 4 K.

## II. EXPERIMENTAL METHODS

The nc-Gd samples were prepared by inert-gas condensation of 98.6 at.% $^{160}$Gd as described elsewhere.[19] Each 8-mm diameter, 300-$\mu$m thick disk was held between two 0.5-mm thick aluminium plates with 0.5-mm cadmium foil strips used to center and mask the disk to reduce background. The assembly was mounted in a closed cycle fridge with a partial pressure of helium for thermal uniformity. Neutron diffraction measurements were made on the N5 triple-axis spectrometer at the Canadian Neutron Beam Centre, Chalk River. Measurements were made in $\theta - 2\theta$ mode in a conventional Bragg-Brentano geometry. Flat PG(002) crystals were used as the monochromator and analyzer. The elastic properties of the samples were probed in the temperature range 4 to 330 K with a fixed final wavelength of 1.638 Å and collimation settings of [open, 0.8°, 0.55°, open]. A 5-cm-thick pyrolytic graphite (PG) filter was placed after the sample to remove higher-order neutron wavelengths.

The first two allowed reflections from gadolinium [(1 0 0) and (0 0 2)] conveniently provide the information needed to determine the magnitude and direction of the magnetic moment, and at the wavelength used here, they are less than 3° apart, so any absorption correction due to the residual 0.2 at.% $^{155}$Gd and $^{157}$Gd present in the sample, can be neglected as it affects the two peaks equally. For the same reason, thermal-motion corrections were also neglected. We covered the $2\theta$ range 28°–38° so that we also recorded the (1 0 1) reflection as it is stronger than the first two and partially overlaps the (0 0 2) reflection (see Fig. 1). The peak positions, widths, and integrated areas were determined by fitting three Gaussians to the observed patterns. All uncertainties are 1-$\sigma$ intervals unless otherwise noted.

## III. RESULTS

The nuclear-only intensities (i.e., with no magnetic contributions) of the first three diffraction peaks from gadolinium metal ($P6_3/mmc$ #194, $a = b = 3.563$ Å, $c = 5.698$ Å) were calculated using PowderCell[20] for a neutron wavelength of 1.638 Å. No absorption corrections were applied as the diffraction peaks are within a very narrow range of $2\theta$. The calculated intensities normalized to that of the (1 0 1) reflection are shown in Table I, and compared with the measured integrated intensities at 310 K from the three samples studied here. All of the measured intensities are within $2\sigma$ of their expected values, however, there appears to be a systematic drop in the relative intensity of the (0 0 2) reflection as the material is annealed to promote grain growth and produce more coarse-grained samples. This might suggest that there is a tendency for the $c$ axes of the grains to lie preferentially in the plane of the sample, the reverse of that reported in an earlier $^{155}$Gd Mössbauer study,[16] however, there does not appear to be a corresponding change in the relative intensity of the (1 0 0) reflection, nor would this texture be consistent with a more extensive analysis of equivalent samples.[19] We believe that any texture that might be present is weak, and since we will be normalizing all magnetic signals to the observed nuclear scattering, any bias that might be introduced by weak texture will cancel, at least to first order.

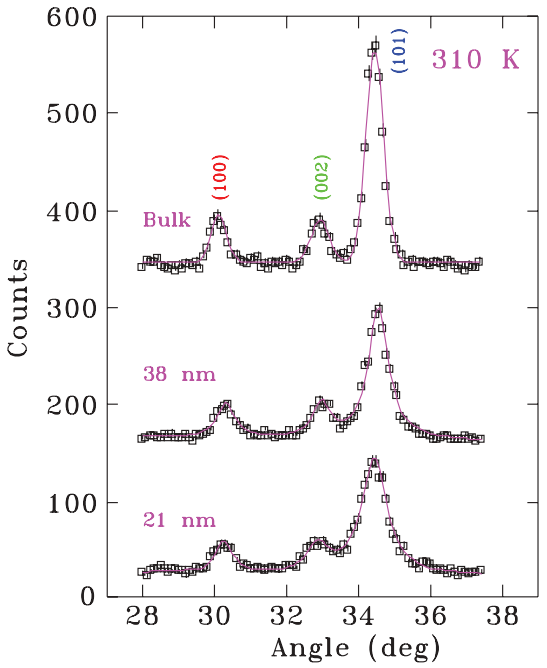


FIG. 1. (Color online) Neutron diffraction patterns taken at 310 K (above $T_c$) for the three $^{160}$Gd metal samples studied here. The patterns have been offset vertically for clarity. Solid lines show fits to three Gaussian peaks.

As gadolinium metal orders ferromagnetically, the magnetic scattering occurs only at nuclear-allowed positions and so it simply adds to the existing nuclear peaks. Following Cable and Wollan[4] we note that the ratio of the magnetic ($I_{\mathrm{mag}}$) to nuclear ($I_{\mathrm{nuc}}$) scattering intensities at a given Bragg peak depends on a number of parameters that are either constant (e.g., the nuclear scattering length) or effectively constant over the narrow angular range relevant here (e.g., the magnetic form factor for $Gd^{3+}$). The two important exceptions are the relative magnetization ($\sigma/\sigma_0$) and an angular term ($q_{(hkl)}$) that

TABLE I. Calculated powder diffraction intensities for the first three peaks in the gadolinium diffraction pattern normalized to that of the (1 0 1) reflection. The experimental values measured at 310 K for the three samples studied here are also shown.

| | Intergrated intensity | | | |
|---|---|---|---|---|
| Reflection | Calculated | Bulk | 38 nm | 21 nm |
| (1 0 0) | 0.187 | 0.192(14) | 0.200(15) | 0.191(19) |
| (0 0 2) | 0.232 | 0.199(14) | 0.255(17) | 0.280(27) |
| (1 0 1) | 1.000 | – | – | – |

takes account of the moment direction and scattering vector. Gathering the (effectively) constant terms together ($K$) we can write the normalized magnetic intensity ($R_{(hkl)}$) as

$$R_{(hkl)} = \frac{I_{\rm mag}}{I_{\rm nuc}} = K\, q^2_{(hkl)}\, (\sigma/\sigma_0)^2$$

and if $\phi_c$ is the angle between the magnetization and the $c$ axis, then

$$\langle q^2\rangle_{(100)} = 1 - \tfrac{1}{2}\sin^2\phi_c$$

($\langle\cdots\rangle$ denotes an average over possible orientations within the basal plane) and

$$q^2_{(002)} = \sin^2\phi_c.$$

From these expressions it is clear that a magnetic contribution to the (1 0 0) peak is present for any orientation of the moment, but that the (0 0 2) contribution vanishes if the moments are parallel to the $c$ axis (i.e., for $\phi_c = 0$). Thus the onset of ordering can be detected through an increase in the (1 0 0) reflection, no matter which way the moments point, and an increase in the (0 0 2) reflection unambiguously indicates that the moments are *not* parallel to the $c$ axis. Finally, the relationship

$$\left(R_{(100)} + \tfrac{1}{2}R_{(002)}\right) \propto (\sigma/\sigma_0)^2$$

can be used to follow the total magnetization.

It is clear from Fig. 1 that the diffraction peaks from the two nanocrystalline samples are much broader than those from the reference sample. If we assume that the width of the (1 0 1) reflection from the reference sample represents the instrumental resolution, then the additional width of the corresponding peaks for the nc-Gd samples can be used to obtain estimates of the particle sizes, using the simple Scherrer formula. This method yields 21.2 ± 1.4 nm and 46.7 ± 4.5 nm, in agreement with the more complete Williamson-Hall x-ray characterization[21] carried out during the preparation of the samples.

### A. Reference sample

Cooling the reference sample to 6 K leads to substantial increases in the intensities of the (1 0 0) and (1 0 1) reflections as the 7 $\mu_B$ Gd moments order. There is a much smaller, but nonzero, change at the (0 0 2) position, suggesting that the moments are fairly close to, but not parallel to the $c$ axis, as expected.

Tracking the integrated intensities as a function of temperature and normalizing to the nuclear-only intensity recorded at 310 K (Fig. 2) shows that a magnetic contribution to the (1 0 0) and (1 0 1) peaks appears as soon as the sample orders at 290(4) K, but that the (0 0 2) reflection only starts to increase in intensity below $T_{sr} = 229(2)$ K as the moments cant away from the $c$ axis. The subsequent increase and then decrease in the (0 0 2) intensity reflects the progressive canting of the moments followed by their rotation back towards the $c$ axis.

The results of combining the magnetic intensity at the (1 0 0) and (0 0 2) reflections to obtain the canting angle ($\phi_c$) and the normalized magnetization [$(\sigma/\sigma_0)^2$] are shown in Fig. 3. The onset points and general behavior are in broad agreement with the earlier results of Cable and Wollan,[4]

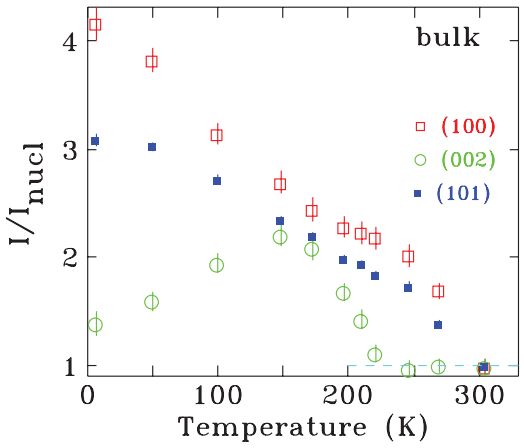


FIG. 2. (Color online) Temperature dependence of the normalized integrated intensities for the coarse-grained "bulk" reference sample of $^{160}$Gd metal showing the onset of order at 290(4) K and the subsequent canting of the moments away from the $c$ axis below $T_{sr} = 229(2)$ K.

however, our canting angle is never as large as theirs; it appears to peak 20–25 K lower in temperature and our $T \to 0$ angle is only 20(1)°, compared to their value of 32°. The consistent behavior of the magnetization through the canting and subsequent return towards the $c$ axis evident in the lower panel of Fig. 3 suggests that any effects of the possible texture apparent in Table I were small and that the normalization to the nuclear intensities corrected for any residual effects. We therefore conclude that the derived $\phi_c(T)$ in Fig. 3 is correct. As will be shown below, the difference between our trend and that reported earlier[4] is not

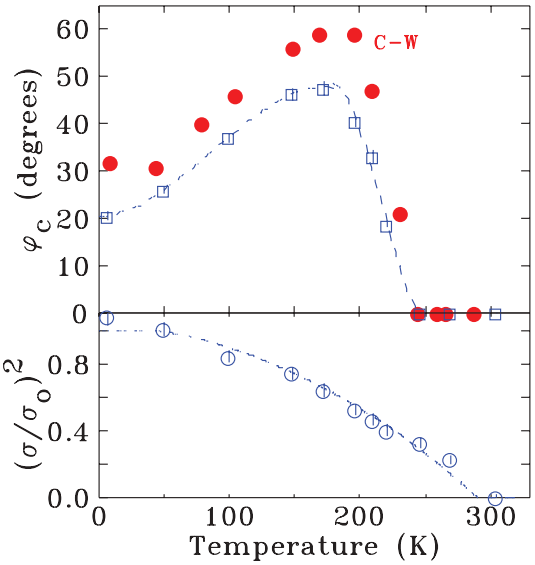


FIG. 3. (Color online) Top: Temperature dependence of the canting angle ($\phi_c$) for the coarse-grained "bulk" reference sample of $^{160}$Gd metal (open symbols) compared with the original results of Cable and Wollan (Ref. 4) (solid symbols, traced from their Fig. 3). The dashed line is a guide to the eye. Bottom: Temperature dependence of the normalized magnetization [$(\sigma/\sigma_0)^2$]. The dashed line is a fit with a $J = \frac{7}{2}$ Brillouin function giving $T_c = 290(4)$ K.

consistent with the effects of a reduced grain size, nor is it likely that the strain effects are significant as the reference sample was prepared by annealing a nc-Gd sample to promote grain growth. It is possible that light element impurities (e.g., C, N, O) introduced during the preparation might be affecting the canting behavior. Light element impurities are often understated but can have significant impacts on the magnetic behavior of rare-earth metals[22] and intermetallic compounds.[23] We note also that to the best of our knowledge, the original 1968 work that was performed on a small (5-mm diameter, 0.5-mm thick) crystal at 0.353 Å has not been repeated on a modern thermal instrument with one of the large single crystals of $^{160}$Gd that are now available.

### B. Nanocrystalline samples

Two nc-Gd samples with 21- and 38-nm grain sizes were measured and analyzed in the same way as the coarse-grained reference sample. A comparison of the three diffraction patterns taken at 4 K reveals that the (1 0 0):(0 0 2) intensity ratio is smaller in both of the nc-Gd samples than it is in the reference material. It is therefore immediately clear that the gadolinium moments make a much larger angle with the *c* axis in nc-Gd than in the reference sample.

The temperature dependence of the normalized intensity (Fig. 4) shows that unlike the reference case (Fig. 2), a magnetic contribution appears at both the (1 0 0) and (0 0 2) positions at the *same* temperature, and that the intensities track together to about 50 K before separating. Thus, the initial ordering in the nc-Gd samples is not along the *c*-axis as it is in the reference sample, and the angle between the

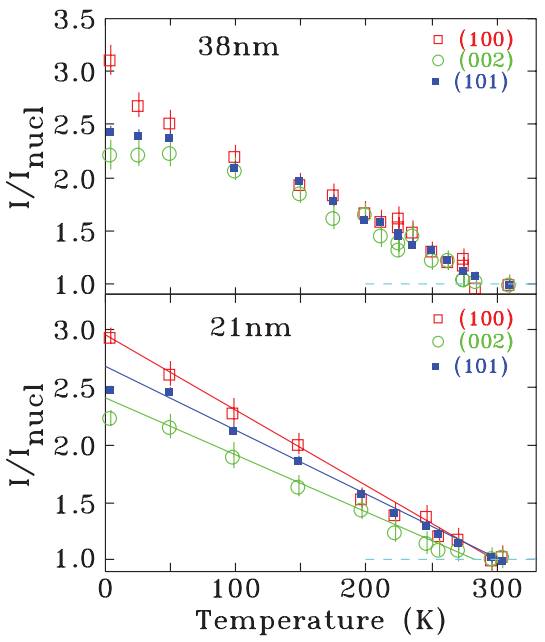


FIG. 4. (Color online) Temperature dependence of the normalized integrated intensities for the 38- (top) and 21-nm (bottom) nc-Gd samples. In both cases the (1 0 0) and (0 0 2) show a single onset temperature and increase together, with only a weak deviation from this trend visible in the data for the 38-nm sample below 50 K. The solid lines are linear fits to the 21-nm data that serve to emphasize the common trends in all three signals.

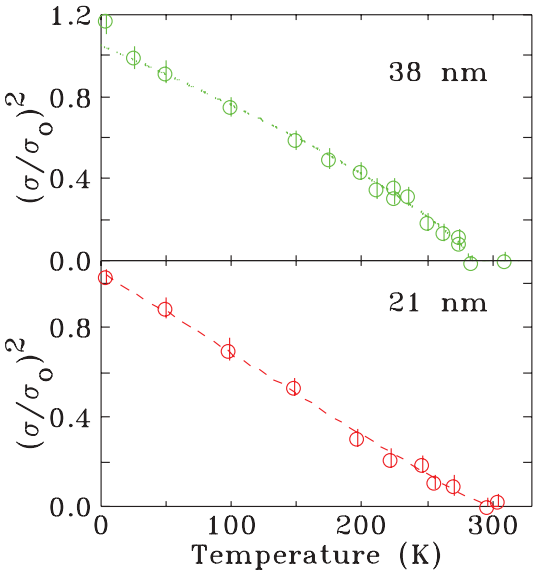


FIG. 5. (Color online) Temperature dependence of the normalized magnetization $[(\sigma/\sigma_0)^2]$ for the 38- (top) and 21-nm (bottom) nc-Gd samples. Dashed lines are power-law fits described in the text and serve primarily as guides to the eye.

moments and the *c* axis remains approximately constant on cooling. Linear fits to the 21-nm data, shown in Fig. 4, give onset temperatures of 298(11) and 283(5) K for the (1 0 0) and (0 0 2) reflections, respectively; consistent both with each other and with the 301(4) K onset for the (1 0 1) reflection. A similar analysis of the 38-nm data gives 302(5) and 290(5) K for the (1 0 0) and (0 0 2) reflections, respectively, with 295(2) K for the (1 0 1) reflection. The possible gaps in onset [12(7) K, 38 nm and 15(12) K, 21 nm] are hardly significant, do not show a grain-size trend, and are far smaller than the ∼60 K gap seen in the reference sample.

$(\sigma/\sigma_0)^2$ derived from the magnetic intensity at the (1 0 0) and (0 0 2) positions is shown in Fig. 5 for the two nc-Gd samples. It is apparent that the temperature dependence is flatter than that seen in the reference sample (Fig. 3), and attempts to fit even a classical ($J = \infty$) Brillouin function did not work well. A power law of the form

$$I = I_0 \left(1 - \frac{T}{T_c}\right)^{2\beta}$$

reproduces the observed trends with $\beta = 0.37(1)$ for the 38-nm sample and 0.50(5) for the 21-nm sample. The latter trend is linear, as seen for each of the contributing peaks in Fig. 4. This behavior indicates that the thermal demagnetization of the nc-Gd samples is dominated by a broad spectrum of low-lying collective excitations, rather than the local spin reversals that lead to the $J = \frac{7}{2}$ Brillouin behavior seen in the reference sample. It is likely that the extensive spin disorder seen in SANS studies[17–19] is the source of these excitations. The spin disorder due to defects in the grain boundary layer was found to exhibit a characteristic length scale of about 5 nm,[17,19] far larger than the ∼1-nm grain boundary itself, and reflecting a significant perturbation of the spin system, presumably carried by the exchange interactions.

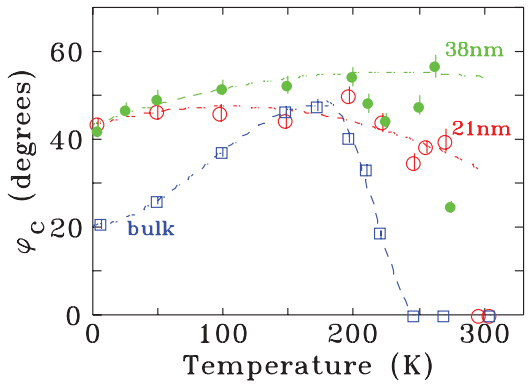


FIG. 6. (Color online) Temperature dependence of the canting angle ($\phi_c$) for the three samples studied here: • 38 nm, ◯ 21 nm, □ bulk reference sample (shown for comparison). Dashed lines are guides to the eye.

A second consequence of the spin disorder noted in the SANS studies is a reduction in the magnetization by about 3% at 5 K in 9 tesla[17,19] for the particle sizes used here. Two disorder contributions were identified in the SANS work: the intragrain disorder due to grain boundary effects noted above, and the random orientation of the individual grains and their easy magnetization axes. Both are suppressed by an applied field, but the approach to saturation is slow.[17] Since we are working with a powder, our diffraction measurements are not affected by the second effect, however, intragrain disorder will reduce the effective gadolinium moment as it occurs on short length scales. The estimates for $\sigma_0$ derived from the fits shown in Fig. 5 are consistent with each other but are only 85(3)% of the value for the reference sample. This 15(3)% reduction is far larger than the ∼3% seen by magnetization,[17,19] however, the magnetization value only represents the residual disorder that could not be suppressed by an external field of 9 tesla, whereas our 15(3)% reduction was observed in zero applied field and reflects the impact of all intragrain spin disorder.

It is unlikely that the moment reduction is spatially uniform across the grains and most of the observed reduction in the average moment derived from neutron diffraction is probably due to the highly disordered grain boundaries which contribute little to our measured magnetic intensity. A core-shell picture of the magnetism in nc-Gd would imply that the coherent magnetic scattering from the ferromagnetically ordered gadolinium cores comes from a smaller volume than the crystallographic grains that contribute to the nuclear scattering. This model is supported by the observation that all three peaks for both nc-Gd samples studied here are *broader* at 3 K than they are at 310 K. No such broadening is observed for the reference sample: All three peak widths at 6 K are within 1-$\sigma$ of their values at 310 K (two of the three actually fit as sharper). Using the (1 0 1) reflection as it is the most intense, and subtracting the signal at 310 K to remove the nuclear contribution, yields a magnetic "grain size" 6(2)-nm smaller than the crystallographic grain size. This suggests that there is a ∼3-nm-thick shell of disordered moments on the surface of each grain, consistent with the correlation length for the disorder scattering derived from SANS.[17–19]

Finally, we turn to the ordering direction in nc-Gd. As shown in Fig. 3, bulk gadolinium orders with its moments parallel to the $c$ axis at 293 K and then the moments cant away by up to 50° (this work), or 60° (Ref. 4) below 230 K. The behavior of the nc-Gd magnetic order is quite different. Figure 6 shows that neither nc-Gd sample exhibits $c$-axis ordering at any temperature, and that the canting angle ($\phi_c$) is largely temperature independent at ∼50° for both samples. There is a weak trend to smaller canting angles on cooling (stronger in the 38-nm sample) but the trends seen in our reference sample (Fig. 2) and single-crystal gadolinium[4] are clearly absent. While the behavior is likely driven by a combination of spin disorder from defects in the grain boundaries and internal pressures induced by interface stresses from high-angle grain boundaries, we emphasize that the coherent magnetic scattering used to determine $\phi_c$ comes primarily from the ordered *cores* of the grains. The few-Å spin-spin correlation lengths in the magnetically disordered shell regions[17–19] lead to small-angle scattering that appears only at very low angles ($2\theta < 5°$). This is well outside the range covered here, and does not affect our results. The trends in $\phi_c$ reflect the behavior of the ferromagnetically ordered moments in the cores of the nanocrystalline grains.

## IV. CONCLUSION

Nanocrystalline gadolinium orders ferromagnetically with the moments canted by about 50° away from the $c$ axis. This canting angle is largely independent of temperature in contrast to the more complex behavior seen in bulk gadolinium. In addition, the temperature dependence of the total magnetization showed strong departures from the expected $J = \frac{7}{2}$ Brillouin function, reflecting the impact of grain boundary disorder on the magnetic excitations. We can rule out impurities as the origin of the differences in magnetic behavior as a bulk reference sample, prepared from an initially nanocrystalline starting sample by annealing to coarsen the grain structure, exhibited conventional bulk behavior.

## ACKNOWLEDGMENTS

Financial support for various stages of this work was provided by the Natural Sciences and Engineering Research Council of Canada and Fonds Québécois de la Recherche sur la Nature et les Technologies. JMC acknowledges support from the University of New South Wales, Australia. We thank the Deutsche Forschungsgemeinschaft (Project No. MI 738/3-2) and the National Research Fund of Luxembourg (ATTRACT Project No. FNR/A09/01) for financial support.

[1] M. Colarieti-Tosti, S. I. Simak, R. Ahuja, L. Nordström, O. Eriksson, D. Åberg, S. Edvardsson, and M. S. S. Brooks, Phys. Rev. Lett. **91**, 157201 (2003).

[2] G. Will, R. Nathans, and H. A. Alperin, J. Appl. Phys. **35**, 1045 (1964).

[3] S. N. Kaul and S. Srinath, Phys. Rev. B **62**, 1114 (2000).

[4]J. W. Cable and E. O. Wollan, Phys. Rev. **165**, 733 (1968).
[5]W. D. Corner and B. K. Tanner, J. Phys. C **9**, 627 (1976).
[6]O. Hartmann, R. Wäppling, E. Karlsson, G. Kalvius, L. Asch, F. Litterst, K. Aggarwal, K. Münch, F. Gygax, and A. Schenck, Hyperfine Interact. **64**, 369 (1991).
[7]H. Klimker and M. Rosen, Phys. Rev. B **7**, 2054 (1973).
[8]H. Bartholin and D. Bloch, J. Phys. Chem. Solids **29**, 1063 (1968).
[9]D. D. Jackson, V. Malba, S. T. Weir, P. A. Baker, and Y. K. Vohra, Phys. Rev. B **71**, 184416 (2005).
[10]J. J. M. Franse and R. Gersdorf, Phys. Rev. Lett. **45**, 50 (1980).
[11]C. G. Granqvist and R. A. Buhrman, J. Appl. Phys. **47**, 2200 (1976).
[12]J. Weissmüller, A. Michels, D. Michels, A. Wiedenmann, C. E. Krill, H. M. Sauer, and R. Birringer, Phys. Rev. B **69**, 054402 (2004).
[13]C. E. Krill, F. Merzoug, W. Krauss, and R. Birringer, Nanostruct. Mater. **9**, 455 (1997).
[14]R. Birringer, M. Hoffmann, and P. Zimmer, Phys. Rev. Lett. **88**, 206104 (2002).
[15]D. Michels, C. E. Krill, and R. Birringer, J. Magn. Magn. Mater. **250**, 203 (2002).
[16]R. Kruk, M. Ghafari, H. Hahn, D. Michels, R. Birringer, C. E. Krill, R. Kmiec, and M. Marszalek, Phys. Rev. B **73**, 054420 (2006).
[17]F. Döbrich, M. Elmas, A. Ferdinand, J. Markmann, M. Sharp, H. Eckerlebe, J. Kohlbrecher, R. Birringer, and A. Michels, J. Phys.: Condens. Matter **21**, 156003 (2009).
[18]A. Michels, F. Döbrich, M. Elmas, A. Ferdinand, J. Markmann, M. Sharp, H. Eckerlebe, J. Kohlbrecher, and R. Birringer, Europhys. Lett. **81**, 66003 (2008).
[19]F. Döbrich, J. Kohlbrecher, M. Sharp, H. Eckerlebe, R. Birringer, and A. Michels, Phys. Rev. B **85**, 094411 (2012).
[20]W. Kraus and G. Nolze, J. Appl. Crystallogr. **29**, 301 (1996).
[21]H. P. Klug and L. E. Alexander, *X-Ray Diffraction Procedures for Polycrystalline and Amorphous Materials* (Wiley, New York, 1974), Chap. 9.
[22]K. A. Gschneidner, Jr., J. Alloys Compd. **193**, 1 (1993).
[23]Y. Mudryk, D. Paudyal, V. K. Pecharsky, and K. A. Gschneidner, Phys. Rev. B **85**, 014116 (2012).